Water Splitting Hot Paper

Deutsche Ausgabe: DOI: 10.1002/ange.201600525
Internationale Ausgabe: DOI: 10.1002/anie.201600525

Hierarchical $NiCo_2O_4$ Hollow Microcuboids as Bifunctional Electrocatalysts for Overall Water-Splitting

Xuehui Gao[+], Hongxiu Zhang[+], Quanguo Li, Xuegong Yu, Zhanglian Hong, Xingwang Zhang, Chengdu Liang, and Zhan Lin**

Abstract: *Bifunctional electrocatalysts for the oxygen evolution reaction (OER) and hydrogen evolution reaction (HER) in alkaline electrolyte may improve the efficiency of overall water splitting. Nickel cobaltite ($NiCo_2O_4$) has been considered a promising electrode material for the OER. However, $NiCo_2O_4$ that can be used as an electrocatalyst in HER has not been studied yet. Herein, we report self-assembled hierarchical $NiCo_2O_4$ hollow microcuboids for overall water splitting including both the HER and OER reactions. The $NiCo_2O_4$ electrode shows excellent activity toward overall water splitting, with 10 mA cm^{-2} water-splitting current reached by applying just 1.65 V and 20 mA cm^{-2} by applying just 1.74 V across the two electrodes. The synthesis of $NiCo_2O_4$ microflowers confirms the importance of structural features for high-performance overall water splitting.*

As fossil fuels decline and environmental pollutions aggravate, future societies will have to rely on sustainable and regenerative energy sources for development. Water splitting has been widely regarded as a promising and sustainable approach of producing clean hydrogen fuel from aqueous solutions.[1] However, the practical applications of water splitting are very limited because splitting reactions, including the anodic oxygen evolution reaction (OER) and the cathodic hydrogen evolution reaction (HER), are strongly uphill with large overpotentials.[2] In alkaline solution, noble-metal oxides (e.g. Ir oxides)[3] usually serve as the OER catalysts and NiMo alloy are traditional electrocatalysts for HER.[4] However, their large-scale applications are restricted by the high cost of precious metals.[5] It is highly desired to design effective catalysts for water splitting by using non-noble metals. In this regard, transition-metal oxides, chalcogenides, and phosphides have been demonstrated as promising electrocatalysts for the OER and HER reactions in water splitting.[1b,6]

[*] X. H. Gao,[+] Prof. X. G. Yu, Prof. Z. L. Hong
State Key Laboratory of Silicon Materials, School of Materials Science and Engineering, Zhejiang University, Hangzhou 310027 (China)
H. X. Zhang,[+] Q. G. Li, Prof. X. W. Zhang, Dr. C. D. Liang, Prof. Z. Lin
Key Laboratory of Biomass Chemical Engineering of Ministry of Education, College of Chemical and Biological Engineering
Zhejiang University
Hangzhou 310027 (China)
E-mail: xwzhang@zju.edu.cn
zhanlin@zju.edu.cn

[+] These authors contributed equally to this work.

Supporting information for this article can be found under: http://dx.doi.org/10.1002/anie.201600525.

Among non-noble-metal-based electrocatalyst materials, mixed oxides, especially nickel cobaltite ($NiCo_2O_4$), have received considerable interest as they have shown electrocatalytically active for OER,[7] owing to their low cost, abundance, good electrical/ionic conductivity, and rich redox reactions.[8] To our knowledge, however, $NiCo_2O_4$ that can catalyze hydrogen evolution efficiently in alkaline solution has not been reported to date. It would be a great advance if $NiCo_2O_4$ can be used as a state-of-the-art electrocatalyst for full water splitting.

Hierarchical three-dimensional (3D) materials with mesoporous structures and hollow interiors have been widely designed for applications in electrochemical reactions.[9] The complex structures endow materials with high specific surface areas that facilitates diffusion of active species and accelerates subsequent surface reactions as compared to on bulk solid structures.[10] When applying one-dimensional (1D) nanostructures in electrocatalysis, the contact surface between electrolyte and catalyst is enhanced. Nanostructures that promote the release of evolved gas bubbles and exhibit maximum catalytic performance have been demonstrated.[11] Therefore, it is of great interest to synthesize electrochemically active materials with hierarchical 3D hollow structures that consist of 1D nanostructures, which make them promising electrode materials for both the HER and OER in water splitting.

Herein, we report hierarchical $NiCo_2O_4$ hollow microcuboids, constructed by 1D nanowires, as bifunctional electrocatalysts for both the HER and OER as well as overall water splitting. These novel hierarchical $NiCo_2O_4$ hollow microcuboids show excellent catalytic activity and stability towards overall water splitting. For example, the current density of 10 mA cm^{-2} current was reached by applying just 1.65 V, while the current density of 20 mA cm^{-2} was obtained by applying just 1.74 V across the two electrodes. The synthesis of $NiCo_2O_4$ microflowers for comparison further confirms the importance of structural features for high-performance water splitting. All of these results make hierarchical $NiCo_2O_4$ hollow microcuboids excellent electrode materials for practical applications in overall water splitting.

Hierarchical $NiCo_2O_4$ hollow microcuboids were obtained via a thermally driven conversion process (Figure 1). The Ni–Co based precursor was first grown into hollow microcuboids with good uniformity using a solvothermal method, and they served as sacrificial templates for the hierarchical $NiCo_2O_4$ hollow microcuboids. A subsequent annealing treatment in air at 350 °C with a ramping rate of 1 °C min^{-1} for 2 h was applied to transform the Ni–Co based precursor into $NiCo_2O_4$ hollow microcuboids.

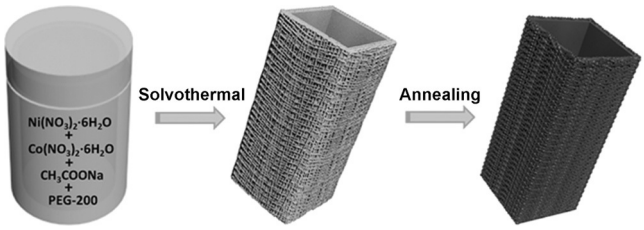

Figure 1. Schematic representation of the formation of hierarchical $NiCo_2O_4$ hollow microcuboids.

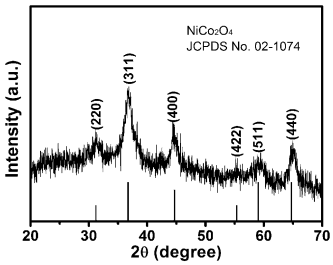

Figure 3. XRD patterns of hierarchical $NiCo_2O_4$ hollow microcuboids.

The crystallographic structure and phase purity of the as-obtained sample were first examined by powder X-ray diffraction (XRD) analysis (Figure S1, see the Supporting Information), which can be assigned to nickel–cobalt hydroxide hydrate. The morphology and structure of the as-obtained Ni–Co based precursor are characterized by using scanning electron microscopy (SEM), as shown in Figure S2. A panoramic SEM image shows that the precursors are uniform hollow microcuboids with an average length of approximately 10 μm (Figure S2a). The magnified SEM images (Figures S2b–S2d) further reveals that these hollow microcuboids are assembled from 1D nanowires. After annealing in the air at 350 °C, the precursors are converted into $NiCo_2O_4$ with well-retained hollow microcuboid morphology (Figures 2a and 2b). As confirmed by the peaks in the XRD in Figure 3, the diffraction patterns are attributed to $NiCo_2O_4$ (JCPDS card No. 02-1074). Their hollow interiors and detailed geometrical structure were further elucidated by TEM (Figure 2c), which duplicated well the size and shape of precursor Ni–Co hollow microcuboids. The magnified TEM image (Figure 2d) clearly shows the hollow microcuboid is composed of 1D nanowires with mesopores distributed throughout the shell. As determined by N_2 sorption measurement (Figure S3), these $NiCo_2O_4$ hollow microcuboids have a relatively high Brunauer–Emmett–Teller (BET) surface area of 69.6 $m^2 g^{-1}$ with pore size of 17.43 nm. Figure 2e shows high-resolution TEM image of a hollow microcuboid, in which an interplanar spacing of 0.245 nm and 0.287 nm is assigned to the (311) and (220) lattice plane of $NiCo_2O_4$, respectively. The selected-area diffraction (SAED) pattern for hierarchical $NiCo_2O_4$ hollow microcuboids (Figure 2f) indicates high crystallinity, and each diffraction ring is also well indexed to $NiCo_2O_4$. The hollow microcuboids contain two types of porosities: the mesopores that can be measured by the BET theory, and the macropores as the hollow interior. Such a hierarchical hollow structure holds great promise in offering sufficient surface area to facilitate electrochemical reactions and efficient penetration of electrolyte into active materials.[10a] The chemical compositions and oxidation states of $NiCo_2O_4$ were investigated by X-ray photoelectron spectra (XPS; Figure S4), showing the existence of Co–O and Ni–O bonds.

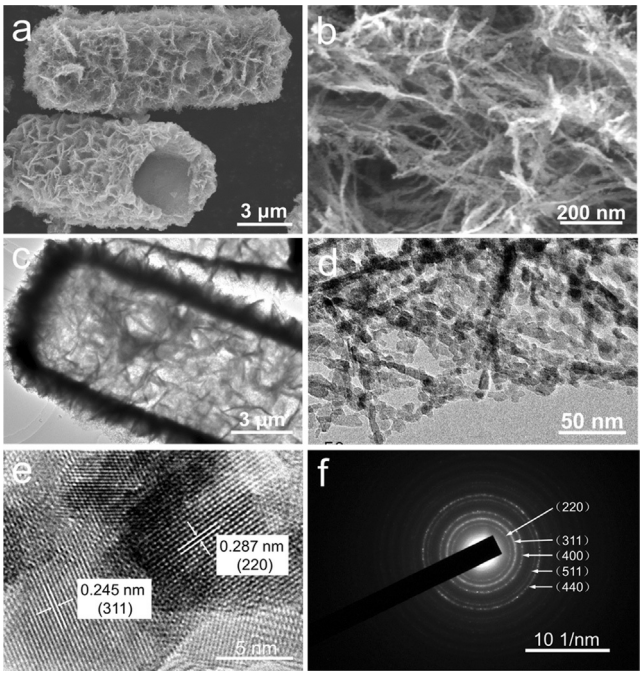

Figure 2. a,b) FESEM, c) a low and d) a high magnification TEM images, e) a HRTEM image, and f) corresponding SAED pattern of hierarchical $NiCo_2O_4$ hollow microcuboids.

The electrocatalytic activities of hierarchical $NiCo_2O_4$ hollow microcuboids for HER were evaluated with a three-electrode electrochemical cell in 1.0 M NaOH solution (see the Supporting Information). Figure 4a shows the polarization curve after *iR* correction of the $NiCo_2O_4$ hollow microcuboids with a scan rate of 3 $mV s^{-1}$. The $NiCo_2O_4$ hollow microcuboids exhibit a low onset potential (−50 mV, $J = -1.0\ mA cm^{-2}$) and a rapidly rising current density with applied potential. The onset potential compared favorably to most of recently reported earth-abundant HER electrocatalysts (see comparisons in Table S1). The overpotential required to drive cathodic current density of 10 and 100 $mA cm^{-2}$ are −110 and −245 mV, respectively. The excellent electrocatalytic activity of microcuboids is further confirmed by the low Tafel slope. Generally, there are two mechanisms involving the HER process in alkaline media. The HER pathway could be through the Volmer–Heyrovsky process [Eq. (1)] or Volmer–Tafel pathways [Eq. (2)].[12]

$$\begin{aligned} &H_2O + e^- \rightarrow H_{ads} + OH^- \text{ (Volmer)} \\ &H_{ads} + H_2O + e^- \rightarrow H_2 + OH^- \text{ (Heyrovsky)} \end{aligned} \quad (1)$$

$$\begin{aligned} &H_2O + e^- \rightarrow H_{ads} + OH^- \text{ (Volmer)} \\ &H_{ads} + H_{ads} \rightarrow H_2 \text{ (Tafel)} \end{aligned} \quad (2)$$

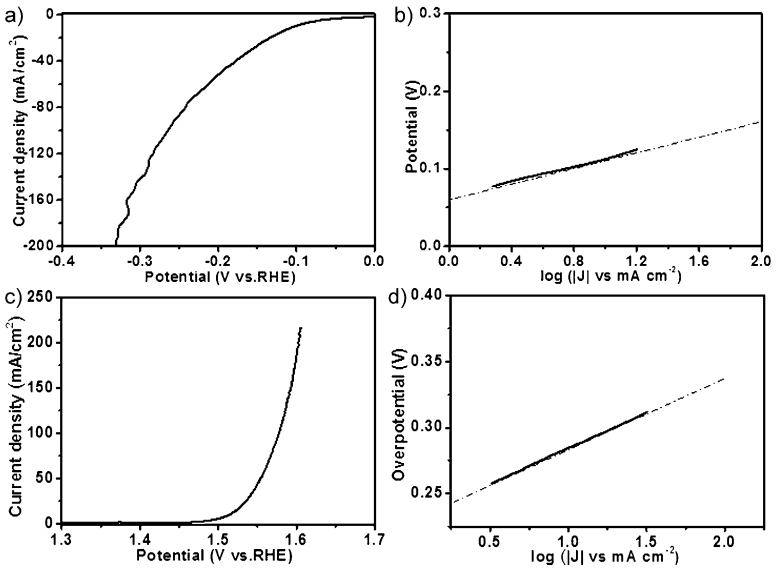

Figure 4. a) Polarization curve and b) Tafel plot of hierarchical $NiCo_2O_4$ hollow microcuboids for HER. c) Polarization curve and d) Tafel plot of $NiCo_2O_4$ hollow microcuboids for OER.

Depending upon whether the Volmer, Heyrovsky, or Tafel component is the rate-limiting step, a slope of 120, 40, or 30 mV decade^{-1} should be observed, respectively. As shown in Figure 4b, the Tafel value of $NiCo_2O_4$ microcuboids was 49.7 mV decade^{-1}, which suggest that the HER over $NiCo_2O_4$ hollow microcuboids proceeded by a Volmer–Heyrovsky mechanism and the Heyrovsky reaction was the rate-limiting step. The Tafel slope of the $NiCo_2O_4$ hollow microcuboids is relatively small in alkaline solution compared with most of metal oxide electrocatalysts reported (see Table S1). The performance is even close to that of CoPS, a high-performance Earth-abundant catalyst measured in acidic electrolyte (0.5 M H_2SO_4) for HER.[13] We further investigated the electrode kinetics by electrochemical impedance spectroscopy (EIS); and the small charge-transfer resistance indicated a fast charge-transfer rate (Figure S5). We also measured the value of double-layer capacitance (C_{dl}), which was proportional to effective active surface area of $NiCo_2O_4$ (Figures S6 and S7). The electrocatalytic performance of $NiCo_2O_4$ hollow microcuboids might be attributed to their particular mesoporous structure and ultrahigh surface area as discussed above.

We also investigated the OER performance of $NiCo_2O_4$ hollow microcuboids in 1.0 M NaOH solution. The polarization curve after *iR* correction showing the geometric current density (*J*) plotted against applied potential of $NiCo_2O_4$ sample are exhibited in Figure 4c. $NiCo_2O_4$ hollow structures produced a small onset potential of 1.46 V (J = 1.0 mA cm^{-2}) and an anode current density of 10 mA cm^{-2} at a potential of 1.52 V. These data indicated that hierarchical $NiCo_2O_4$ hollow microcuboids have a good catalytic activity for the OER. The high electrochemical activity of $NiCo_2O_4$ is attributed to its unique hollow mesoporous structure composed of 1D nanowires, which offers more accessible active surface areas for permeation of electrolyte to improve the OER activity.[14] The superior OER activity of the hierarchical $NiCo_2O_4$ hollow microcuboids is confirmed by their small Tafel slope of 53 mV decade^{-1} (Figure 4d). Such a Tafel slope is amongst in the smallest reported for ternary metal oxide catalysts for the OER. The kinetics of the electrode was also investigated by the EIS measurement as shown in Figure S8. For comparison, the OER performance of the Ni-foam substrate was also measured and the results are inferior to those of the $NiCo_2O_4$ (Figures S9 and S10). The electrochemical parameters of recently reported congeneric OER catalysts in alkaline media are also listed for comparison in Table S2, which further confirm that the OER performance of hierarchical $NiCo_2O_4$ hollow microcuboids are comparable to or better than most reported electrocatalysts. In addition, metal hydroxides forming on the surface of metal oxides might also contribute to the catalysis for the OER.[15]

Stability is an important parameter to evaluate the quality of the catalyst. The stability tests for both HER and OER were evaluated separately by continuous galvanostatic measurement for 32 h. The $NiCo_2O_4$ catalyst gave a good level of stability with the overpotential no more than 15 mV during 32 h continuous galvanostatic electrolysis at -10 mA cm^{-2} as shown in Figure 5a (lower curve), indicating good durability

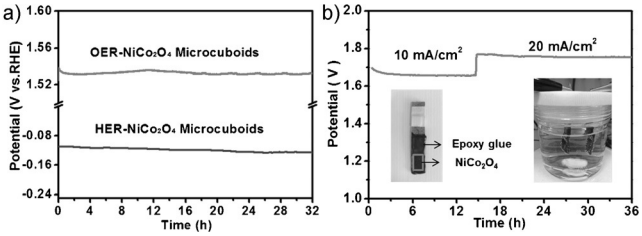

Figure 5. a) Galvanostatic measurement of OER and HER by $NiCo_2O_4$ hollow microcuboids in 1 M NaOH at a current density of 10 mA cm^{-2} and -10 mA cm^{-2}, respectively. b) Overall water-splitting characteristics in a two-electrode configuration at current densities of 10 and 20 mA cm^{-2}; Inset in (b) shows optical image of $NiCo_2O_4$ electrode and overall water-splitting device.

of hierarchical $NiCo_2O_4$ hollow microcuboids towards HER in alkaline solution. The stability for OER was also evaluated by galvanostatic measurement at a continuous electrocatalytic current density of 10 mA cm^{-2} for 32 h (Figure 5a, top curve). The overpotential increased only 10 mV over 32 h. The durable performance demonstrated that the $NiCo_2O_4$ structures are stable and practical electrocatalysts for OER.

For the measurement of the catalytic activity toward overall water-splitting, a two-electrode configuration was investigated and hierarchical $NiCo_2O_4$ hollow microcuboids were prepared as electrode materials for both the anode and the cathode. Overall water-splitting characteristics in a two-electrode configuration at current densities of 10 and 20 mA cm^{-2} are shown in Figure 5b. The hierarchical

$NiCo_2O_4$ hollow microcuboid structure electrode showed excellent activity, with 10 mA cm^{-2} water-splitting current reached by applying just 1.65 V and 20 mA cm^{-2} by just 1.74 V across the two electrodes. Furthermore, the potential was very stable and retained for at least 36 h. The hierarchical $NiCo_2O_4$ hollow microcuboid structure gives low overpotentials, which demonstrates their promising practical applications for full water splitting.

To demonstrate the importance of structure features for high-performance water splitting, $NiCo_2O_4$ microflowers were synthesized for comparison (see the Supporting Information) to the $NiCo_2O_4$ hollow microcuboids. The crystallographic structure and phase purity of the microflower sample examined by XRD confirm the synthesis of $NiCo_2O_4$ (Figure S11, JCPDS card No. 02-1074). The morphology and structure of the as-obtained $NiCo_2O_4$ are characterized by using SEM, which show high uniformity of these $NiCo_2O_4$ microflowers assembled from nanoplates (Figure S12). These $NiCo_2O_4$ microflowers have a relatively low BET surface area of 32.1 m^2 g^{-1} with pore size of 3.82 nm (Figure S13). The polarization curve and Tafel plot of $NiCo_2O_4$ microflowers for HER are shown in Figures S14,S15. $NiCo_2O_4$ microflower electrodes demonstrate much higher cathodic overpotential of 190 mV and larger Tafel slope of 130.5 mV decade^{-1}. The polarization curve and Tafel plot of the $NiCo_2O_4$ microflowers for OER are also shown in Figures S16,S17. $NiCo_2O_4$ microflower electrodes have a much higher onset potential of above 1.50 V and larger Tafel slope of 67.8 mV decade^{-1} compared to those of $NiCo_2O_4$ hollow microcuboids. All these data indicate the superior electrocatalytic activities of hierarchical $NiCo_2O_4$ hollow microcuboids for both the HER and OER reactions than those of $NiCo_2O_4$ microflowers.

The superior catalytic performance of hierarchical $NiCo_2O_4$ hollow microcuboids in overall water splitting are ascribed to the synergistic effects of their 1D nanowire mesh structure and unique 3D hierarchical hollow structures. The nanowire and hollow structures provide a large active surface area, which facilitates diffusion of active species and accelerates subsequent surface electrochemical reactions. Benefiting from these unique 3D hierarchical structures, the reaction kinetics of both the HER and OER are significantly promoted. Well-defined 1D nanowires and mesoporous hollow structures provide smooth pathways to facilitate penetration of the electrolyte and enlarge the contact surface between reactants and active sites. Furthermore, 3D hierarchical hollow structures assembled from 1D nanowires enables facile release of evolved gas bubbles to further improve the reaction interface.

In summary, we report, for the first time, the synthesis of hierarchical $NiCo_2O_4$ hollow microcuboids constructed by 1D porous nanowire subunits, and our study shows the opportunities offered by these novel structures to function as highly active and stable electrode materials for high-performance overall water splitting. The $NiCo_2O_4$ electrode shows excellent activity toward overall water splitting, with 10 mA cm^{-2} water-splitting current reached by applying just 1.65 V and 20 mA cm^{-2} by just 1.74 V across the two electrodes. The hierarchical $NiCo_2O_4$ hollow microcuboid structure decreases overpotentials greatly, suggesting their promising practical applications for full water splitting. The facile preparation of $NiCo_2O_4$ hollow microcuboids allows large-scale production of advanced bifunctional electrocatalysts for overall water splitting. The synthesis of $NiCo_2O_4$ microflowers for comparison further confirms the importance of structural features for high-performance water splitting. The uniform hollow microcuboid structures might be the basis for designing other mixed metal oxides as high-performance electrode materials for a broad range of electrochemical applications, such as batteries, supercapacitors, and electrocatalysis.

Acknowledgements

Z.L. thanks funding from Chinese government under the "Thousand Youth Talents Program" and from Zhejiang Province Science Fund for Distinguished Young Scholars (Project LR16B060001). This work is also supported by the Natural Science Foundation of China (Project No. 21522606) and by the Fundamental Research Funds for the Central Universities.

Keywords: electrochemistry · $NiCo_2O_4$ · solvothermal synthesis · water splitting

How to cite: *Angew. Chem. Int. Ed.* **2016**, *55*, 6290–6294
Angew. Chem. **2016**, *128*, 6398–6402

[1] a) D. S. Kong, J. J. Cha, H. T. Wang, H. R. Lee, Y. Cui, *Energy Environ. Sci.* **2013**, *6*, 3553; b) Z. Peng, D. Jia, A. M. Al-Enizi, A. A. Elzatahry, G. F. Zheng, *Adv. Energy Mater.* **2015**, *5*, 1402031.

[2] a) T. Liu, Q. Liu, A. M. Asiri, Y. Luo, X. Sun, *Chem. Commun.* **2015**, *51*, 16683; b) J. Wang, W. Cui, Q. Liu, Z. Xing, A. M. Asiri, X. Sun, *Adv. Mater.* **2016**, *28*, 215.

[3] H. N. Nong, H. S. Oh, T. Reier, E. Willinger, M.-G. Willinger, V. Petkov, D. Teschner, P. Strasser, *Angew. Chem. Int. Ed.* **2015**, *54*, 2975; *Angew. Chem.* **2015**, *127*, 3018.

[4] a) M. G. Walter, E. L. Warren, J. R. McKone, S. W. Boettcher, Q. Mi, E. A. Santori, N. S. Lewis, *Chem. Rev.* **2010**, *110*, 6446; b) M. S. Faber, S. Jin, *Energy Environ. Sci.* **2014**, *7*, 3519; c) M. Zeng, Y. Li, *J. Mater. Chem. A* **2015**, *3*, 14942.

[5] H. Zhu, J. F. Zhang, R. P. Yan Zhang, M. L. Du, Q. F. Wang, G. H. Gao, J. D. Wu, G. M. Wu, M. Zhang, B. Liu, J. M. Yao, X. W. Zhang, *Adv. Mater.* **2015**, *27*, 4752.

[6] a) L. L. Feng, G. T. Yu, Y. Y. Wu, G. D. Li, H. Li, Y. H. Sun, T. Asefa, W. Chen, X. X. Zou, *J. Am. Chem. Soc.* **2015**, *137*, 14023; b) J. Bao, X. D. Zhang, B. Fan, J. J. Zhang, M. Zhou, W. L. Yang, X. Hu, H. Wang, B. C. Pan, Y. Xie, *Angew. Chem. Int. Ed.* **2015**, *54*, 7399; *Angew. Chem.* **2015**, *127*, 7507; c) H. T. Wang, H. W. Lee, Y. Deng, Z. Y. Lu, P. C. Hsu, Y. Y. Liu, D. C. Lin, Y. Cui, *Nat. Commun.* **2015**, *6*, 7261; d) M. Ledendecker, S. Krick Calderón, C. Papp, H. P. Steinrück, M. Antonietti, M. Shalom, *Angew. Chem. Int. Ed.* **2015**, *54*, 12361; *Angew. Chem.* **2015**, *127*, 12538.

[7] a) Y. G. Li, P. Hasin, Y. Y. Wu, *Adv. Mater.* **2010**, *22*, 1926; b) S. Chen, S. Z. Qiao, *ACS Nano* **2013**, *7*, 10190; c) H. N. Nong, H. S. Oh, T. Reier, E. Willinger, M. G. Willinger, V. Petkov, D. Teschner, P. Strasser, *Angew. Chem. Int. Ed.* **2015**, *54*, 2975.

[8] a) D. P. Dubal, P. Gomez-Romero, B. R. Sankapal, R. Holze, *Nano Energy* **2015**, *11*, 377; b) J. Zhou, Y. Huang, X. Cao, B. Ouyang, W. Sun, C. Tan, Y. Zhang, Q. Ma, S. Liang, Q. Yan, H. Zhang, *Nanoscale* **2015**, *7*, 7035.

[9] a) R. Schreiber, J. Do, E.-M. Roller, T. Zhang, V. J. Schüller, P. C. Nickels, J. Feldmann, T. Liedl, *Nat. Nanotechnol.* **2014**, *9*, 74; b) K. Miszta, J. de Graaf, G. Bertoni, D. Dorfs, R. Brescia, S. Marras, L. Ceseracciu, R. Cingolani, R. van Roij, M. Dijkstra, *Nat. Mater.* **2011**, *10*, 872.

[10] a) X. H. Gao, G. Li, Y. Y. Xu, Z. L. Hong, C. D. Liang, Z. Lin, *Angew. Chem. Int. Ed.* **2015**, *54*, 14331; *Angew. Chem.* **2015**, *127*, 14539; b) X. H. Gao, H. B. Wu, L. X. Zheng, Y. J. Zhong, Y. Hu, X. W. Lou, *Angew. Chem. Int. Ed.* **2014**, *53*, 5917; *Angew. Chem.* **2014**, *126*, 6027; c) F. X. Ma, L. Yu, C. Y. Xu, X. W. Lou, *Energy Environ. Sci.*, **2016**, *9*, 862.

[11] a) X. J. Liu, J. F. Liu, Y. P. Li, Y. J. Li, X. M. Sun, *ChemCatChem* **2014**, *6*, 2501; b) J. M. Wang, Y. M. Zheng, F. Q. Nie, J. Zhai, L. Jiang, *Langmuir* **2009**, *25*, 14129; c) M. S. Faber, R. Dziedzic, M. A. Lukowski, N. S. Kaiser, Q. Ding, S. Jin, *J. Am. Chem. Soc.* **2014**, *136*, 10053.

[12] a) M. A. Domínguez-Crespo, A. M. Torres-Huerta, B. Brachetti-Sibaja, A. Flores-Vela, *Int. J. Hydrogen Energy* **2011**, *36*, 135; b) E. Skúlason, V. Tripkovic, M. E. Björketun, S. Gudmundsdóttir, G. Karlberg, J. Rossmeisl, T. Bligaard, H. Jónsson, J. K. Nørskov, *J. Phys. Chem. C* **2010**, *114*, 18182.

[13] M. Cabán-Acevedo, M. L. Stone, J. Schmidt, J. G. Thomas, Q. Ding, H. C. Chang, M. L. Tsai, J. H. He, S. Jin, *Nat. Mater.* **2015**, *14*, 1245.

[14] G. H. Yu, L. B. Hu, M. Vosgueritchian, H. L. Wang, X. Xie, J. R. McDonough, X. Cui, Y. Cui, Z. Bao, *Nano Lett.* **2011**, *11*, 2905.

[15] a) H. Liang, F. Meng, M. Cabán-Acevedo, L. Li, A. Forticaux, L. Xiu, Z. Wang, S. Jin, *Nano Lett.* **2015**, *15*, 1421; b) Z. Zhao, H. Wu, H. He, X. Xu, Y. Jin, *Adv. Funct. Mater.* **2014**, *24*, 4698.

Received: January 18, 2016
Published online: April 8, 2016

